Hindawi Publishing Corporation
Advances in OptoElectronics
Volume 2011, Article ID 368327, 6 pages
doi:10.1155/2011/368327

Research Article

Modelling of Output Statistics of Single and $\mathcal{M}$-Mode Straight and Curved Er^{3+}:Ti:$LiNbO_3$ Waveguide Amplifiers

Niculae N. Puscas

Physics Department I, Faculty of Applied Science, University "Politehnica" of Bucharest, Splaiul Independentei 313, 060042 Bucharest, Romania

Correspondence should be addressed to Niculae N. Puscas, pnt@physics.pub.ro

Received 29 April 2011; Accepted 20 July 2011

Academic Editor: Xian Cao

A theoretical analysis of some statistical parameters which characterize the Er^{3+}-doped Ti:$LiNbO_3$ single and $\mathcal{M}$-mode straight and curved waveguides is presented in this paper. In the derivation and the evaluation of the spectral optical quality factor, the power spectral density, the Fano factor, the statistical fluctuation, and the spontaneous emission factor we used the small gain approximation, and the photon statistics master equation of the linear amplifier (considering that the photon number distribution is determined by the normalized mode intensity profiles which are not uniform in the transversal section of the waveguide), transposed to the case of straight and curved amplifiers. The simulation results show the evolution of the above-mentioned parameters under various pump regimes and waveguide lengths.

1. Introduction

Lithium niobate photonic circuits permit the generation, transmission, and processing of photons to be accommodated on a single chip. Compact photonic circuits with multiple components integrated on a single chip are crucial for efficiently implementing quantum information processing schemes.

The study of the noise spectral distribution and the output statistics in a system where coherent and chaotic (thermal) fields are superimposed plays an important role in obtaining integrated amplifiers with low noise and high optical gain. This is the reason why, over the last decade, a great attention has been devoted to the analysis of the statistical properties of Er^{3+}-doped fibres and waveguide amplifiers [1–12].

A novel technique for evaluating the output statistics of single and $\mathcal{M}$-mode straight and curved Er^{3+}-doped Ti:$LiNbO_3$ amplifiers, like the spectral optical quality factor, the power spectral density, the output mean photon number, the statistical fluctuation, the Fano factor, and the spontaneous emission factor, is proposed in this paper. The reason of this analysis is related to the fact that often in the waveguides is excited not only the fundamental mode but also other high-order ($\mathcal{M}$) modes [11, 13], which influence the output gain, noise figure, signal-to-noise ratio, and the statistical properties of the waveguide.

The paper is organized as follows. Section 2 is devoted to the basic equations used to evaluate the population of the upper atomic energy level and the evolution of the pump, signal, power spectral density, Amplified Spontaneous Emission (ASE), the Fano factor, the statistical fluctuation, and the spontaneous emission factor which characterize the output statistics of the single and $\mathcal{M}$-mode waveguides. Also, in this section the model used for the calculation of optical field distribution in the bent waveguides is presented [6–11]. Section 3 deals with the discussion of the computed results, while the conclusion of this work is presented in Section 4.

2. Theoretical Considerations

The quantum theory of the statistical properties in the optical waveguide amplifiers is based on the more general quantum theories of coherent light, coherent light/matter interaction, noise, and laser oscillations [1, 8–11]. We used the two-level model to describe the above-mentioned processes [1, 8–11]. The transitions between the two lowest energetic level manifolds of the Er^{3+} ions incorporated

into the $LiNbO_3$ lattice determine absorption and optical amplification by stimulated emission in the range 1440 nm < λ < 1640 nm. The optical amplification of a signal wave takes place if the population inversion with respect to the ground state $^4I_{15/2}$ is achieved after the optical pumping to a pump band (an excited state) followed by a fast relaxation to the metastable level $^4I_{13/2}$. Using a pump radiation having λ = 1484 nm it is possible to neglect the excited state absorption (ESA) and to consider a quasi-two-level model for the simulation of the Er^{3+}-doped Ti : $LiNbO_3$ waveguide amplifiers in the wavelength range 1440 nm < λ < 1640 nm.

The interaction of pump/signal photons with Er^{3+} ions can be represented using the rate Equations [8–11]. In the case of the steady state regime by discretizing the considered frequency spectrum in a number of intervals $\Delta\nu$ small enough so that the frequency-dependent quantities can be assumed constant over each of them, one obtains the equations for the pump, signal, and ASE evolution after integration over the waveguide transversal cross-section in the form [8–11]

$$\begin{aligned}\frac{d}{dz}P_{km}^{\pm}(z) &= \pm\Bigg\{\Bigg[(\sigma_{e,km}+\sigma_{a,km})\int_A N_2(x,y,z)\,i_m(x,y)\,dx\,dy \\ &\quad -\left(\sigma_{a,km}\int_A N_2(x,y,z)\,i_m(x,y)\,dx\,dy+\alpha_{km}\right)\Bigg] \\ &\quad \times P_{km}^{\pm}(z)+h\nu_k\Delta\nu\sigma_{e,km}\int_A N_2(x,y,z)\,i_m(x,y)\,dx\,dy\Bigg\},\end{aligned} \tag{1}$$

where $P_{km}^{\pm}(z)$ represent the power in the spectral interval $\Delta\nu$ around frequency ν_k, for the polarization m in the forward (+) and backward (−) propagation directions, with x and y being the coordinates in the plane perpendicular to the waveguide axis z and N_2 is the steady state solution of the rate equations for the upper populations of the two levels which is written in the form

$$\begin{aligned}N_2(x,y,z) &= N_{T0}\,d(x,y) \\ &\quad\times\frac{\sum_{k,m}(\tau/h\nu_k)\sigma_{a,km}\left(P_{km}^{+}(z)+P_{km}^{-}(z)\right)i_m(x,y)}{1+\sum_{k,m}(\tau/h\nu_k)(\sigma_{a,km}+\sigma_{e,km})\left(P_{km}^{+}(z)+P_{km}^{-}(z)\right)i_m(x,y)}.\end{aligned} \tag{2}$$

In (2) the Er^{3+} ions distribution in the waveguide has been written in the form $N_T(x,y) = N_{T0}d(x,y)$, where $N_{T0} = N_T(0,0)$ and $d(x,y)$ is the normalized dopant distribution. Similar notations have been used for the cross-sections, $\sigma_{a,m}(\nu)$ and $\sigma_{e,m}(\nu)$ for the optical waveguide losses α_{km}. The term $h\nu_k\Delta\nu$ in (1) represents an equivalent spontaneous emission input noise power in the frequency slot $\Delta\nu$ corresponding to the frequency ν_k [1].

Spontaneous transitions from the excited states to the ground state are taken into account by the rate $A_{21} = 1/\tau$, τ being the fluorescence lifetime of the Er^{3+} ions. The absorption and emission rates of the amplified spontaneous emission are W_{12}^{ASE} and W_{21}^{ASE}, respectively.

The energy fine structure is taken into account by wavelength-dependent absorption and emission cross-sections. The cross-sections profiles constitute the basis for the computation of the gain, noise figure, and other parameters which characterize the amplifiers. The pump (signal) absorption, and emission rates are $R_{12}(W_{12})$ and $R_{21}(W_{21})$, respectively. To analyse the behaviour of the amplifier in terms of signal gain, pump absorption and ASE output power, it is convenient to distinguish in the optical power at frequency ν_k the coherent contribution due to injected signal or pump beams (stimulated emission or absorption) from the incoherent one due to the (amplified) spontaneous emission. We can do this by observing that the forcing term in (1) contributes only to the incoherent ASE power and by using different "k" indexes for the two kinds of contribution. The stimulated transition rates due to the pump, signal, and ASE fields can be written in terms of the corresponding field intensities $I_m(x,y,z,\nu)$, the absorption and emission cross-sections, $\sigma_{a,m}(\nu)$ and $\sigma_{e,m}(\nu)$, and the photon energies $h\nu$ [1, 8]:

$$\begin{aligned}R_{12}, W_{12}, W_{12}^{\mathrm{ASE}} &= \sum_{m=\mathrm{TE,TM}}\int\sigma_{a,m}(\nu)\frac{I_m(x,y,z,\nu)}{h\nu}\,d\nu, \\ R_{21}, W_{21}, W_{21}^{\mathrm{ASE}} &= \sum_{m=\mathrm{TE,TM}}\int\sigma_{e,m}(\nu)\frac{I_m(x,y,z,\nu)}{h\nu}\,d\nu.\end{aligned} \tag{3}$$

In (1)–(3) the index m allows to distinguish the two polarizations sides of the guided field. Moreover, the optical intensities can be expressed as the product of a power spectral density $P_m(x,y)$ and the normalized field intensities $i_m(x,y)$, which can be assumed constant in the frequency range of interest.

The boundary conditions for (1) can be written in the form

$$\begin{aligned}P_{km}^{+}(z=0) &= (1-R_{0,km})P_{in0,km}+R_{0,km}P_{km}^{-}(z=0), \\ P_{km}^{-}(z=L) &= (1-R_{L,km})P_{inL,km}+R_{L,km}P_{km}^{+}(z=L),\end{aligned} \tag{4}$$

where $R_{0,km}, R_{L,km}$ are the input and output reflectivities and $P_{in0,km}, P_{inL,km}$ are the optical powers injected at $z = 0$ or at $z = L$. We assume that the signal is injected only from the section $z = 0$ and that no noise power is entering the amplifier (i.e., $P_{in0,km} = P_{inL,km} = 0$ for the ASE beams). By properly choosing the values of R_0 and R_L we can account for the natural reflectivities of the $LiNbO_3$-air interface, as well as analyse the case of a wavelength-selective coating; moreover, if we set R_L to a high value (approx. 100%), our model can describe the behavior of a double-pass amplifier for the pump and the signal. For the numerical integration of the system of equations (1)-(2) in our model we took into account the overlap between the normalized field intensity

and the (normalized) dopant distribution and the (normalized) upper laser level population by introducing the corresponding overlap integrals $\Gamma_{T,m}$ and $\Gamma_{2,m}$, respectively,

$$\Gamma_{T,m}(z) = \int_A d(x,y)\, i_m(x,y)\, dx\, dy, \tag{5}$$

$$\Gamma_{2,m}(z) = \frac{1}{N_{T0}} \int_A N_2(x,y,z)\, i_m(x,y)\, dx\, dy. \tag{6}$$

The effects of gain saturation due to the amplified signal or to the ASE power are accounted for in the expression for the population N_2: as the signal and ASE power grows the emission rate increases and N_2 decreases, leading to a reduction of $\Gamma_{2,m}$ and consequently of the gain factor $a_{km}\Gamma_{2,m}$ in (1).

Considering a collection of atoms with population density distribution $N_1(x,y,z)$ for the ground state and $N_2(x,y,z)$ for the excited state, the rate of change of the probability for having n photons at frequency ν in a single longitudinal mode (P_n) is given by the *photon statistics master equation* of the linear amplifier [1].

Assuming that the normalized mode intensity profiles $i_m(x,y)$ are not uniform in the transversal section of the waveguide the photon number distribution becomes $n \times i_m(x,y)$. Multiplying the photon statistics master equation by $i_m(x,y)$ and integrating over the transversal section of the waveguide we obtain the following [9]:

$$\begin{aligned}\frac{dP_n(z,\nu)}{dz} &= \gamma_e(z,\nu) n P_{n-1}(z,\nu) + \gamma_a(z,\nu) n P_{n+1}(z,\nu) \\ &\quad - [\gamma_e(z,\nu)(n+1) + \gamma_a(z,\nu) n] P_n(z,\nu),\end{aligned} \tag{7}$$

where

$$\begin{aligned}\gamma_e &= \gamma_e(z,\nu) = \sigma_e(\nu) \int_A N_2(x,y,z)\, i_m(x,y)\, dx\, dy, \\ \gamma_a &= \gamma_a(z,\nu) = \sigma_a(\nu) \int_A N_1(x,y,z)\, i_m(x,y)\, dx\, dy.\end{aligned} \tag{8}$$

In (7) σ_a and σ_e represent the cross-sections for the absorption and emission processes. Furthermore, multiplying (7) by the number of photons, n, and summing over n we obtain the output expression for the photon mean value $\langle n(z)\rangle$:

$$\langle n(z)\rangle = G(z)\langle n(0)\rangle + N(z), \tag{9}$$

where

$$G(z,\nu) = \exp\left\{\int_0^z [\gamma_e(z',\nu) - \gamma_a(z',\nu) - \alpha(\nu)]\, dz'\right\}, \tag{10}$$

$$N(z,\nu) = G(z,\nu) \int_0^z \frac{\gamma_e(z',\nu)}{G(z',\nu)} dz' \tag{11}$$

represent the spectral gain and the ASE photon number, respectively.

For coherent input signals with Poisson's statistics $P_n(0) = (\langle n(0)\rangle^n / n!) e^{-\langle n(0)\rangle}$ being well known that $\sigma^2(0) = \langle n(0)\rangle$. In the case of uniform inversion, when the population densities of the upper and lower levels (N_1 and N_2, resp.) do not depend on the waveguide coordinate z, the variance takes the canonical form:

$$\begin{aligned}\sigma^2(z) &= [G(z)\langle n(0)\rangle + N(z)] \\ &\quad + \lfloor 2G(z)N(z)\langle n(0)\rangle + N^2(z)\rfloor.\end{aligned} \tag{12}$$

As a measure of the gain and the noise characteristics of the waveguide amplifiers, we adopted a quality factor

$$Q(z,\nu) = \frac{G(z,\nu)}{F(z,\nu)}, \tag{13}$$

where

$$F(z,\nu) = \frac{1 + 2N(z,\nu)}{G(z,\nu)} \tag{14}$$

represents the noise figure which quantifies the noise properties of an optical amplifier contributing to the deterioration of the signal-to-noise ratio with a purely shot noise.

As mentioned before spontaneous emission is also present in any amplifier. Small amount of this spontaneous emission gets amplified and comes out along with signal as amplified ASE noise.

The ASE noise is generally modelled as white noise with the power spectral density [12]:

$$S(z,\nu) = n_{\mathrm{sp}}(z,\nu)[G(z,\nu) - 1] \cdot h\nu, \tag{15}$$

where $n_{\mathrm{sp}}(z,\nu)$ represents the spontaneous emission factor and h the Plank's constant. The amplifier output statistics can also be characterised by the Fano factor $f(z) = \sigma^2(z)/\langle n(z)\rangle$ and the statistical fluctuation $e(z) = \sigma(z)/\langle n(z)\rangle$ [1]. For Poisson statistics (coherent light), the Fano factor and the statistical fluctuation correspond to $f = 1$ and $e = (\langle n\rangle)^{-1/2}$, while for Bose-Einstein statistics (incoherent light), they are given by $f = \langle n\rangle + 1$ and $e = (1 + 1/\langle n\rangle)^{-1/2}$.

Assuming an input signal characterised by Poisson statistics, and in the limit of high input signals and high gains, the Fano factor and the statistical fluctuation are given by

$$\begin{aligned}f(z,\nu) &\approx 1 + 2n_{\mathrm{sp}}(z,\nu)[G(z,\nu) - 1], \\ e(z,\nu) &\approx \frac{1}{\sqrt{G(z,\nu)}\langle n(0)\rangle} \left\{1 + 2n_{\mathrm{sp}}(z,\nu)[G(z,\nu) - 1]\right\}^{1/2},\end{aligned} \tag{16}$$

where the spontaneous emission factor is given by

$$n_{\mathrm{sp}}(z,\nu) = \frac{N(z,\nu)}{G(z,\nu) - 1} = \frac{G(z,\nu)}{G(z,\nu) - 1} \int_0^z \frac{\gamma_e(z',\nu)}{G(z',\nu)} dz'. \tag{17}$$

In (16) the factor $[1 + 2G(L,\nu)\int_0^L (\gamma_e(z',\nu)/G(z',\nu))dz']^{1/2}$ characterizes the deviation of the output statistics from Poisson.

Often in the waveguides is excited not only the fundamental mode but also other high-order ($\mathcal{M}$) modes, which influence the output gain, noise figure, and the statistical

properties of the waveguide. The normalized field transversal intensity distribution can be written as [13]

$$i(x,y) = \sum_{j=1}^{M} \eta_j i_j(x,y) \exp\left[i\left(\omega t - \beta_j z\right)\right], \tag{18}$$

where β_j are the propagation constants which are different for different modes because of their velocity [11] and

$$\eta_j = \frac{\iint E_p(x,y) \cdot E_j(x,y)\,dx\,dy}{\sqrt{\iint E_p^2(x,y)\,dx\,dy}\sqrt{\iint E_j^2(x,y)\,dx\,dy}} \tag{19}$$

are the overlap coefficients between the pump optical field, $E_p(x,y)$, and the mode fields, $E_j(x,y)$, excited in the waveguide, which satisfy a normalization condition $\sum_{j=1}^{\mathcal{M}} \eta_j = 1$. In our model we considered that the waveguide is pumped by a radiation having a Gaussian distribution of the field using an optical fiber. The integrals in (19) are extended over the transversal section of the waveguide, with x representing the width and y the depth, respectively.

In order to determine the optical field distribution in the bent waveguides we calculated first the refractive index profiles using the Fick's diffusion law [12]. After that, the optical mode fields were calculated numerically for both TE and TM polarisation using the effective index method presented in papers [7, 14].

3. Discussion of the Simulation Results

The system of coupled first-order differential equations (1)-(2) for the optical power components and the upper population level can only be solved by numerical methods. Moreover, the presence of the boundary conditions (4) at both the extremities of the device requires an iterative procedure of integration: (1) integrate from $z = 0$ to $z = L$ the equations for $P_{km}^{+}(z)$ and assuming $P_{km}^{-}(z) = 0$ in the first iteration; (2) integrate from $z = L$ to $z = 0$ the equations for $P_{km}^{-}(z)$, using the values of $P_{km}^{+}(z)$ found previously; (3) restart from point (1), using for $P_{km}^{-}(z)$ the value found at point (2). The iterations are stopped when the change in $P_{km}^{\pm}(z)$ is smaller than a prescribed value.

A particular care should be taken for the evaluation of $\Gamma_{2,m}(z)$ because this quantity determines the incremental gain in (13) and depends on the actual value of the approximation for $P_{km}^{\pm}(z)$; this implies that, at each step of the forward and backward integration along z, we have to evaluate the integral $\Gamma_{2,m}(z)$. Because of our choice of a Runge-Kutta formula (4th order, 4 stages) as the basic integration method, at each step we should evaluate four times (one for each stage) the overlap integral, within a large expense of computer time. Therefore, we decided to perform the transversal integration only at the first stage at each step, and to use the computed value also for the other three stages; this approximation appears not to have a great influence on the solution and represents a good compromise between accuracy and computation time. In our simulations, the spontaneous emission spectrum is divided into 100 slots which corresponds to a wavelength resolution $\Delta\lambda = 2$ nm in the region 1450–1650 nm.

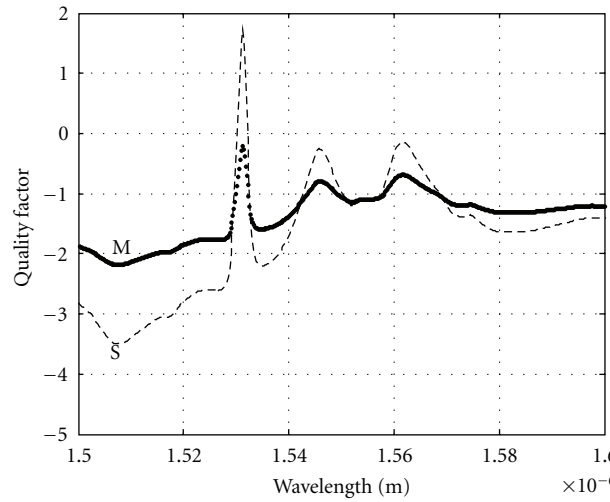

Figure 1: The spectral evolution of the quality factor pass configuration for single (S) and for the $\mathcal{M}$-mode (M) operation.

The intensity profiles $i_m(x,y)$ used in the evaluation of $\Gamma_{2,m}(z)$ and $\Gamma_{T,m}$ are introduced in the model as a set of measured values, while the dopant distribution $d(x,y)$ is approximated by Gaussian, *erfc,* or constant functions in depth (y) and in width (x). The simulation of the optical amplification in Er^{3+}-doped $LiNbO_3$ waveguide has been performed using parameters obtained from the literature [5–10]. Using (1), (2), (10), (11) and (13)–(17) we have calculated numerically the spectral dependence of the quality factor, the power spectral density, the Fano factor, and the statistical fluctuation for a single-pass configuration of the optical amplifier. We assumed a 1484 nm pump and a signal at $\lambda = 1531$ nm, having 1 μW input power.

We used the following values for the absorption (a) and emission (e) cross-sections of the pump (p) and signal (s) for TE and TM polarizations: σ_{TE}^{a} (1484 nm) = $5.61 \times 10^{-25}\,\mathrm{m}^2$, σ_{TM}^{a} (1484 nm) = $3.46 \times 10^{-25}\,\mathrm{m}^2$, σ_{TE}^{e} (1484 nm) = $1.92 \times 10^{-25}\,\mathrm{m}^2$, σ_{TM}^{e} (1484 nm) = $1.105 \times 10^{-25}\,\mathrm{m}^2$, σ_{TE}^{a} (1532 nm) = $17.24 \times 10^{-25}\,\mathrm{m}^2$, σ_{TM}^{a} (1532 nm) = $12.15 \times 10^{-25}\,\mathrm{m}^2$, σ_{TE}^{e} (1532 nm) = $16.36 \times 10^{-25}\,\mathrm{m}^2$, σ_{TM}^{e} (1532 nm) = $11.53 \times 10^{-25}\,\mathrm{m}^2$. The Er-profile has been considered Gaussian in depth and constant in width, with a surface concentration of about $7 \times 10^{25}\,\mathrm{m}^{-3}$ and a diffusion depth of 20 μm and of 5.12 μm in width (defined at $1/e$). We assumed the following values for the scattering loss and spontaneous emission lifetime: $\alpha = 3.7\,\mathrm{dB\cdot m^{-1}}$) for TE, $\alpha = 4.8\ \mathrm{dB\cdot m^{-1}}$ for TM in the case of straight waveguides, and $\alpha = 0.4\,\mathrm{dB\cdot cm^{-1}}$ for TE and TM in the case of the curved ones and $\tau = 2.6$ ms, respectively. The length of the waveguide in our simulations is $L = 5.4$ cm and the pump or signal assumed to be TE polarized if not explicitly stated.

Figure 1 presents the spectral evolution of the quality factor of the signal (13), the signal gain being defined as $G(z) = \ln\lfloor P_{\mathrm{signal}}(z)/P_{\mathrm{signal}}(0)\rfloor$) in the case of single-pass (signal output at $z = L$ with $R(L) = 0$) pass configuration, high pump regime (100 mW incident pump power) for single and for the $\mathcal{M}$-mode operation.

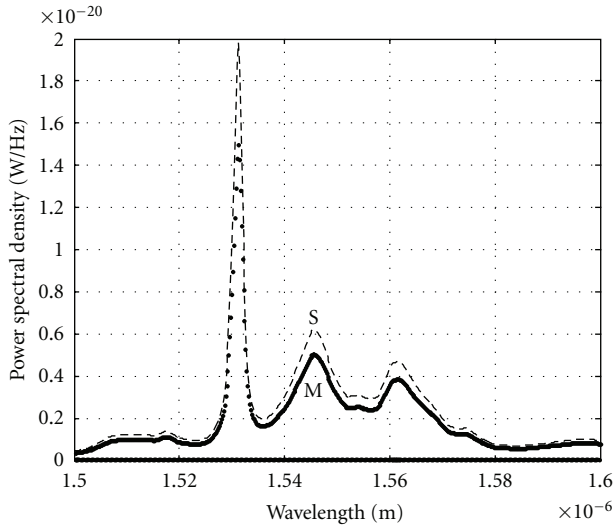

Figure 2: The power spectral density versus wavelength as in Figure 1.

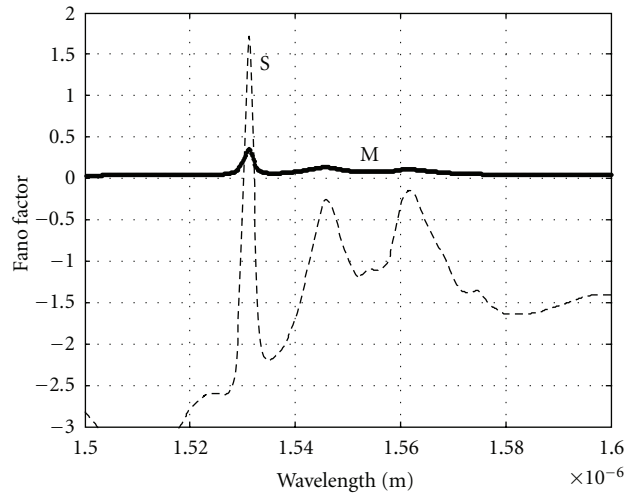

Figure 3: The Fano facto versus wavelength as in Figure 1.

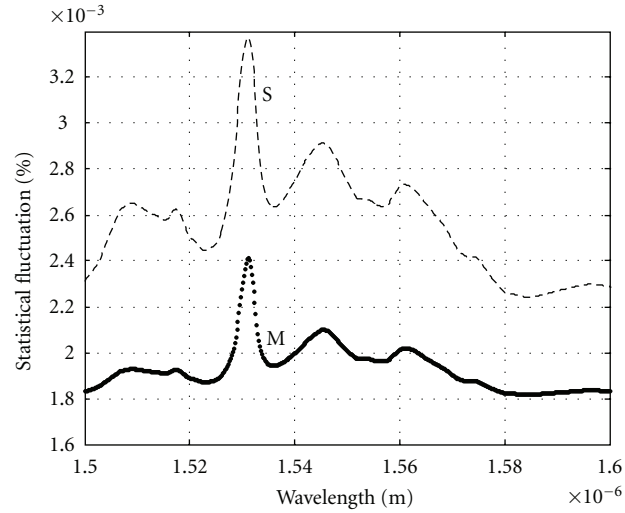

Figure 4: The spectral dependence of the statistical fluctuation as in Figure 1.

As can be seen from Figure 1 the peak values of the quality factor are greater in the single mode operation because the noise figures in the case of $\mathcal{M}$-mode operation are greater than those corresponding to the single one. The $\mathcal{M}$-mode operation in comparison with the single one determines the diminution of the gain and the enhancement of the noise figure because the overlap integral between the population of the excited level and the normalized intensity field profile is smaller in the case of $\mathcal{M}$-mode operation than in the case of the single one (i.e., 1.21 times in the case of Gaussian profile of the dopant for a waveguide having 5.4 cm length and for an input pump power of 100 mW).

Considering a radius of curvature of the waveguide is about 5 cm and its length is 2.5 cm (values commonly used in the laboratories when manufacturing integrated optics Mach-Zehnder interferometers) we obtained a quality factor of about 0.13 for $\lambda = 1.531\,\mu$m.

The power spectral density (Equation (15) is presented in Figure 2). For a high input pump power in the $\mathcal{M}$-mode operation the spontaneous emission factor (which determines the power spectral density) is less than 2 over most of the 60 nm spectral range considered in the figure (i.e., for Gaussian profile of the dopant in the spectral ranges $1.45\,\mu\text{m} \div 1.48\,\mu\text{m}$ and $1.62\,\mu\text{m} \div 1.65\,\mu\text{m}$, which correspond to the amplification of an equivalent input noise of one photon per unit frequency).

In Figures 3 and 4 the spectral dependences of the Fano factor (3) and the statistical fluctuation (4) in single pass configuration are presented.

The dependence of the Fano factor in the case of TE polarization for a signal at $\lambda = 1531$ nm versus the input pump power for a straight waveguide length $L = 5.4$ cm in the single and $\mathcal{M}$-mode operation is presented in Figure 5.

As can be seen form Figure 5 the Fano factor increases rather low with the increasing of the pump power. In the same conditions the statistical fluctuation decreases when the pump power is augmented. This fact confirms that the output statistics is approximately Poissonian for pump powers about 100 mW.

The Fano factor and the statistical fluctuation increase several orders of magnitude with the waveguide length over a range ∼10 cm in both single and $\mathcal{M}$-mode operation. In the case of straight waveguides, the output statistics is approximately Poissonian for waveguide lengths up to 6 cm.

Computing the same parameters in the case of a curved waveguide having a length of about 2.5 cm for the above mentioned conditions we concluded that the photon statistics can be assumed to be Poissonian.

Therefore, it seems that the amplifier length is responsible for the reduction of the Poissonian aspect of the amplified light. This is not the case for shorter waveguide lengths but higher pumping levels, for which the statistical properties of the light are roughly maintained. A consequence concerns

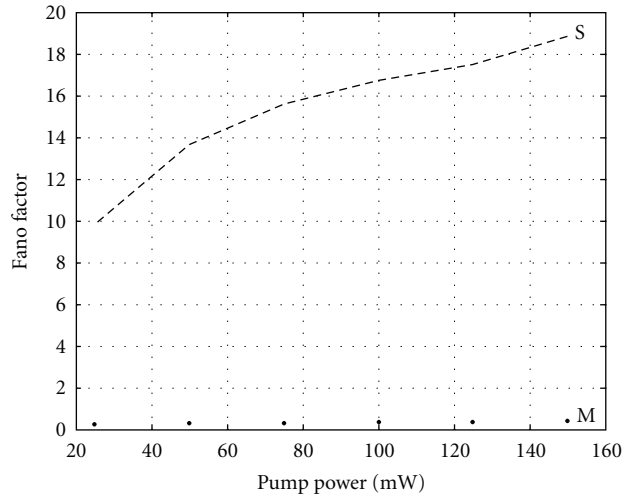

Figure 5: The Fano factor versus the pump power in the single (S) and $\mathcal{M}$-mode (M) operation.

the design of complex structures, when the coherence of the amplified light must be conserved. If the miniaturization of the integrated devices has to be considered, it is preferable to choose short lengths and high-level pumpings, rather than long arms and low pumping regimes.

The above obtained simulated results show that the photon statistics which characterize the Er^{3+}-doped Ti:$LiNbO_3$ waveguide amplifiers (the Fano factor, the statistical fluctuation and the spontaneous emission factor) are correlated with the amplifying phenomena of light (gain, noise figure, signal-to-noise ratio, quality factor).

4. Conclusions

In the small gain approximation an original analysis of the output noise statistical properties of a single and $\mathcal{M}$-mode Er^{3+}-doped $LiNbO_3$ straight and curved waveguide amplifiers has been presented. The simulations concern the quality factor, power spectral factor, Fano factor, and the statistical fluctuation. This analysis demonstrates that the Poissonian photon statistics are maintained for pump powers lower than 100 mW and waveguide lengths smaller than 5 cm for straight waveguides and 2.5 cm in the case of curved ones.

Our simulation results concerning the optical gain, noise figure, and quality factor are in agreement with other experimental and theoretical results [15–17].

The above-mentioned parameters are important when the coherence of the amplified light is an issue for the doped waveguides under investigation. In this paper we have shown that the coherence of the output amplified signal is more sensitive to the waveguide length than to the pumping power. The theoretical results of this simulation characterize the Er^{3+}-doped $LiNbO_3$ waveguide amplifiers from the point of view of noise statistical properties and can be used in the better understanding of the amplification process. Also, they can be used for the design of directional couplers, symmetrical and asymmetrical Mach-Zehnder interferometers, and other complex rare earth-doped integrated circuits.

References

[1] E. Desurvire, *Erbium-Doped Fiber Amplifiers*, Wiley-Interscience, New York, NY, USA, 1994.

[2] P. Diament and M. C. Teich, "Evolution of the statistical properties of photons passed through a traveling-wave laser amplifier," *IEEE Journal of Quantum Electronics*, vol. 28, no. 5, pp. 1325–1334, 1992.

[3] B. E. A. Saleh and M. C. Teich, *Fundamentals of Photonics*, John Wiley & Sons, New York, NY, USA, 2nd edition, 2007.

[4] M. F. Saleh, G. Giuseppe, B. E. A. Saleh, and M. C. Teich, "Modal and polarization qubits in Ti:$LiNbO_3$ photonic circuits for a universal quantum logic gate," *Optics Express*, vol. 18, no. 19, pp. 20475–20490, 2010.

[5] S. Reza, H. Herrmann, R. Ricken, V. Quiring, and W. Sohler, "Spectral characteristics of an integrated tunable frequency shifted feedback laser in erbium doped lithium niobate," in *Proceedings of the 8th International Conference on Optoelectronics, Fiber Optics and Photonics (Photonics '06)*, p. 250, Hyderabad, India, 2006, paper FrA 5.

[6] J. Perina and J. Perina Jr., "Photon statistics of a contradirectional nonlinear coupler," *Quantum and Semiclassical Optics*, vol. 7, no. 5, pp. 849–862, 1995.

[7] G. Lifante, *Integrated Photonics: Fundamentals*, John Wiley & Sons, West Sussex, England, 2003.

[8] N. N. Puscas, D. Scarano, R. Girardi, and I. Montrosset, "Analysis of output statistics of single and double pass Er-doped $LiNbO_3$ waveguide amplifiers," *Optical and Quantum Electronics*, vol. 29, no. 8, pp. 799–809, 1997.

[9] N. N. Puscas, B. Wacogne, A. Ducariu, and B. Grappe, "Modelling the output statistics of Er-doped $LiNbO_3$ curved waveguide amplifiers," *Journal of Modern Optics*, vol. 46, no. 6, pp. 1017–1030, 1999.

[10] N. N. Puscas, "Modelling the spectral noise of single and double pass Er^{3+}-doped Ti:$LiNbO_3$ M-mode straight waveguide amplifiers," *Journal of Optoelectronics and Advanced Materials*, vol. 4, no. 4, pp. 911–921, 2002.

[11] N. N. Puşcaş, "Analysis of the gain and photon ststistics in $^{3+}$Ti:$LiNbO_3$ M-mode straight waveguide amplifiers," *University Politehnica of Bucharest, Scientific Bulletin A*, vol. 65, no. 1, pp. 73–82, 2003.

[12] Y. N. Singh, H. M. Gupta, and V. K. Jain, "Optical amplifiers in broadcast optical networks: a survey," *IETE Technical Review*, vol. 16, no. 5, 6, pp. 449–459, 1999.

[13] I. Turek, I. Martinèek, and R. Stránsky, "Interference of modes in optical fibers," *Optical Engineering*, vol. 39, no. 5, pp. 1304–1309, 2000.

[14] D. Marcuse, *Light Transmission Optics*, Van Nostrand Reinhold, New York, NY, USA, 1972.

[15] R. Brinkmann, I. Baumann, M. Dinand, W. Sohler, and H. Suche, "Er-doped single and double pass Ti:$LiNbO_3$ waveguide amplifiers," *IEEE Journal of Quantum Electronics*, vol. 30, no. 10, pp. 2356–2360, 1994.

[16] J. Guo-Liang, S. Gong-Wang, M. Huan, H. Li-Li, and L. Qu, "Gain and noise figure of a double-pass waveguide amplifier based on Er/Yb-doped phosphate glass," *Chinese Physics Letters*, vol. 22, no. 11, pp. 2862–2869, 2005.

[17] G. Jain, A. Kapoor, and E. K. Sharma, "Er-$LiNbO_3$ waveguide: field approximation for simplified gain calculations in DWDM application," *Journal of the Optical Society of America B*, vol. 26, no. 4, pp. 633–639, 2009.